



Abschlussbericht 30. Dezember 2015

FlexiFuel Combustion

Investigations into Fuel Flexibility at Conditions Typical of Future Large Diesel and Dual-Fuel Engines





WIN GD

Datum: 30.12.2015

Ort: Winterthur

Auftraggeberin:

Bundesamt für Energie BFE
Forschungsprogramm Verbrennung
CH-3003 Bern
www.bfe.admin.ch

Kofinanzierung:

Winterthur Gas & Diesel AG, CH-8401 Winterthur
EU FP-7 (Grant agreement no. 284354)

Auftragnehmer/in:

Winterthur Gas & Diesel AG
Schützenstrasse 1-3
CH-8401 Winterthur
www.wingd.com

Autor:

Andreas Schmid, Winterthur Gas & Diesel AG, andreas.schmid@wingd.com

BFE-Bereichsleitung: Sandra Hermle, sandra.hermle@bfe.admin.ch

BFE-Programmleitung: Stephan Renz, renz.btr@swissonline.ch

BFE-Vertragsnummer: SI/500940

Für den Inhalt und die Schlussfolgerungen sind ausschliesslich die Autoren dieses Berichts verantwortlich.

Bundesamt für Energie BFE

Mühlestrasse 4, CH-3063 Ittigen; Postadresse: CH-3003 Bern
Tel. +41 58 462 56 11 · Fax +41 58 463 25 00 · contact@bfe.admin.ch · www.bfe.admin.ch



Abstract

During the FlexiFuel project, different aspects of spray breakup, atomisation, ignition and combustion have been experimentally investigated with focus on fuel properties and their influence on the above mentioned characteristics. In the Spray Combustion Chamber – itself a result of earlier projects, co-funded by the Swiss Federal Office of Energy and the European Union – the injection of different fuels and different injection parameters have been investigated. To do so, new experimental methods have been developed and successfully applied. The results show large differences between light fuel oils and heavy- or residual fuel oils. The atomisation process of residual fuels is significantly slower, compared to a diesel fuel. Additionally, about 20% of the components in residual fuels do not evaporate under the thermodynamic conditions present at start of injection. The heat of the flame is necessary to evaporate these parts of the fuel in order to ignite them.

Further, possible candidates for alternative fuels were investigated to understand the challenges the application of such fuels might implicate e.g. ignition delay or flame propagation.

The distinct arrangement of the injectors in large marine two-stroke diesel engines lead to asymmetric flow conditions at the orifices of the injector, which raised questions regarding the spray breakup. Investigations showed that spray breakup and spray penetration for injectors of this size are heavily influenced by the in-nozzle flow.

The outcome of the project helps to prepare WinGDs engines for alternative fuels and triggered a series of internal and external follow up projects. One of them with the support of the SFOE: INFLOSCOM.

Zusammenfassung

Während des Flexifuel Projekts wurden verschiedene Aspekte des Strahlaufbruchs, der Atomisierung, Zündung und Verbrennung experimentell untersucht, mit Fokus auf Brennstoffeigenschaften und deren Einfluss auf die oben erwähnten Merkmale. In der Spray Combustion Chamber – ein Resultat früherer Projekte mit Unterstützung vom BFE und der Europäischen Union – wurde die Einspritzung verschiedener Brennstoffe untersucht. Dafür wurden eigens Untersuchungsmethoden entwickelt und erfolgreich angewendet. Die Resultate zeigen grosse Unterschiede zwischen leichten Brennstoffen und Schwerölen. Im Vergleich etwa zu Heizöl extraleicht, haben Schweröle einen signifikant langsameren Aufbruchprozess. Zudem verdampfen gut 20% der Komponenten noch nicht unter den thermodynamischen Bedingungen wie sie im Zylinder während dem Start der Einspritzung herrschen. Die Hitze einer Flamme ist nötig um diese Komponenten restlos zu verdampfen und sie der Verbrennung zuzuführen.

Weiter wurden verschiedene Alternativbrennstoffe untersucht um die Herausforderungen zu verstehen die beim Einsatz solcher Brennstoffe aufkommen könnten, z.B. Einflüsse auf den Zündverzögerung oder die Flammausbreitung.

Die spezielle Anordnung der Einspritzdüsen bei Zweitakt-Grossdieselmotoren führt zu asymmetrischen Strömungsbedingungen in den Spritzlöchern, was Fragen über den Sprayaufbruch aufwarf. Untersuchungen während FlexiFuel zeigten, dass der Strahlaufbruch und die Eindringtiefe des Strahls stark von der Düseninnenströmung beeinflusst werden.

Die Ergebnisse aus dem FlexiFuel Projekt tragen viel zum Verständnis der alternativen Brennstoffe bei und haben weitere interne und externe Nachfolgeprojekte lanciert. Eines davon wieder mit der grosszügigen Unterstützung vom BFE: INFLOSCOM.



Executive summary

The target of FlexiFuel was the investigation of the effect of non-conventional fuels as well as off-specification fuel properties on spray and combustion processes at conditions typical of actual and future large diesel and dual-fuel engines. The well-established and unique Spray Combustion Chamber (SCC) test facility served as the basis for studies of fuel properties and their effects on spray formation and combustion, which were complementary to activities in the context of the fp7-funded HERCULES-C project and preparing developments in the HERCULES-2 project (Workpackage 1, [1]).

The project is the logical consequence and the continuation of the SCC-project (project nr. 103241). Since its commissioning, this unique experimental setup has continuously been improved in several aspects (e.g. optical accessibility, injection system, measurement techniques, etc.) and is a most valuable tool for the investigation of marine fuel sprays at engine like conditions. In view of future goals, associated systems and components around the SCC needed further development to meet the requirements towards increased fuel flexibility:

The injection system was extended towards a time controlled injection system. This allows the application of so called pilot injectors as they are used in dual fuel engines. Additionally custom-made injectors for the conventional liquid fuel operation have been purchased, allowing the high precision control needed for multiple injections.

For the investigation of the in-nozzle flow and its influence on spray morphology, the Mie scattering technique has been applied. It was used to investigate and understand the sprays of eccentric nozzles, as well as defined in-nozzle flow conditions. It showed that the flow patterns forming at the entrance to the spray hole are transported through the orifice and that their influence on spray morphology is significant.

For the measurement of droplet diameters and velocities, the well-proven Phase-Doppler-Anemometry (PDA) was applied. In order to do so, an approach was found to investigate opaque fuels – i.e. residual or heavy fuel oils (HFO). The system was applied for the first time under engine like conditions and revealed the droplet sizes of a light fuel oil in comparison to a standard HFO. The measurements showed that LFO droplets are much faster in the area of the spray where the measurement were performed. It showed that in case of LFO the most droplets are between 5 and 10 μm , compared to 12 to 20 μm for HFO. The largest LFO droplets are about 20 μm , where for HOF they can be more than twice as large.

Ignition and combustion have been investigated for several fuels like HFO, light fuel oil and alternative fuels. One of these alternative fuels was selected to be shown; a second generation biofuel with the potential to replace fossil based fuels in well-defined regions (currently the world wide HFO consumption cannot be replaced by one single fuel). Spray morphology and ignition delay are comparable to standard (HFO) fuels, whereas the flame propagation process along the spray is slowed down to less than 50% compared to a classic fuel.

Regarding the characteristic fuel system of marine two stroke diesel engines, several situations have been reproduced and simulated, in order to better understand the process of spray breakup and atomisation. It showed that the in-nozzle flow has a tremendous influence on spray morphology. Therefore further investigations in this field are planned for the future. Especially when it comes to fuel flexibility with a broader range of fuel properties, the fluid dynamicall processes need to be properly understood.

Based on the investigations during the FlexiFuel project, interesting facts were revealed and presented in reports and presentations within and outside of WinGD. From the author's personal perspective, the FlexiFuel project was a great success leading to several follow-up projects, publications and not to forget the gain of knowledge within the company.



Contents

Abstract	3
Executive summary	4
1 Status Quo	6
2 Goal of the FlexiFuel combustion project	7
3 Concept – The Spray Combustion Chamber	8
4 Methodology	9
4.1 Continuous usage of an established, unique test vehicle	9
4.2 Investigation of the influence of non-conventional fuels.....	9
4.3 Consideration of future requirements for increased fuel flexibility	9
4.4 Extension of the test rig by developing and implementing suitable components and systems...10	
5 Results	10
5.1 Injection process/ Dual-/Multi fuel systems	10
5.2 Droplet sizes and velocity.....	11
5.2.1 Further development measurement techniques	11
5.2.2 Droplet Generation.....	12
5.2.3 Imaging System	12
5.2.4 Determination of the complex refractive index.....	13
5.2.5 Marine Diesel Fuel Droplet Characterization by Means of PDA.....	14
5.2.6 Experimental investigations under engine relevant conditions.....	17
Light fuel oil.....	17
Heavy fuel oil	19
Comparison between LFO and HFO.....	20
5.3 Ignition and Combustion.....	22
5.3.1 Further development Test rig - Adaption of the media separator	22
5.3.2 Ignition and Combustion by means of Spectroscopy	22
5.3.3 Alternative fuels.....	25
5.4 In-nozzle flow (Mie-scattering)	26
6 Discussion, conclusion and outlook	30
7 References	31
8 Publications within the FlexiFuel project	33



1 Status Quo

Large marine diesel engines are already confronted with a broad variety of fuels during their operation. For commissioning and certification they usually are fueled with Marine Diesel Oil (MDO), whereas during normal operation on board all kind of Heavy Fuel Oils (HFO, also called residual fuels) are applied, depending on price and availability. Currently, the global merchant fleet consumes more than 330 million tons of predominantly residual fuel with high sulphur content annually. With fuel costs contributing up to 80% to a ship's daily operating costs, rising fuel prices and decreasing time-chartering rates render the shipping business less profitable, see Figure 1.

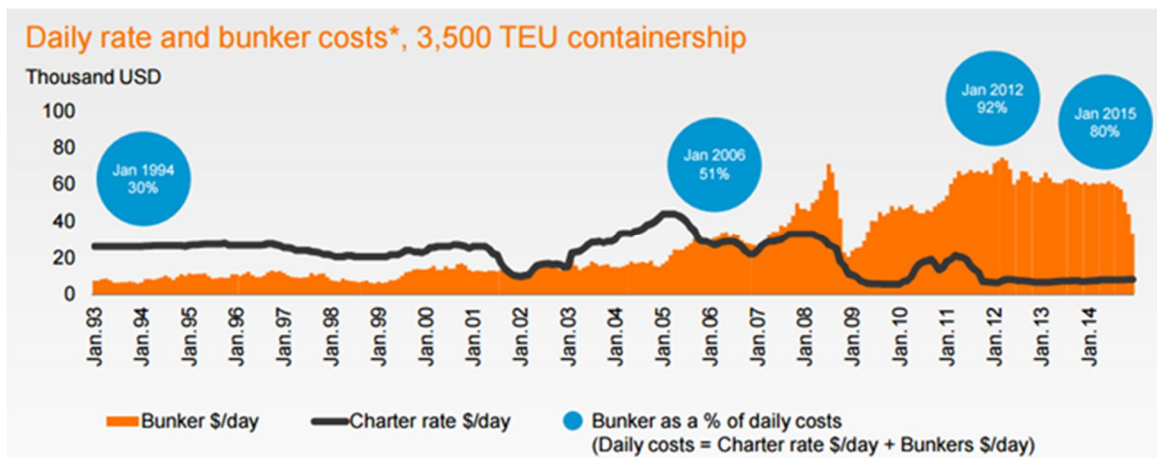


Figure 1: Bunkering costs vs. time charter rates [2]

Emission and fuel quality standards defined in Annex VI of the MARPEC protocol entered into force in 2010 with global limits on the fuels' sulphur content and more stringent regulations applying to designated Emission Control Areas (ECAs). Existing ECAs include the Baltic Sea, the North Sea, coastal zones in Canada and most of the US including Puerto Rico and the US Virgin Islands. Fuel consumption inside ECAs is estimated to 33-55 million tons a year and will rise with implementation of further ECAs. Moreover, NOx emissions are regulated for newly build ships beginning in 2016, putting a limit on the specific emissions as a function of engine speed.

Both regulations provide progressively tightening limits. Compliance options for ship owners can be divided into primary and secondary techniques, with primary techniques aiming at lowering the SOx and NOx emissions at source by e.g. lowering the sulphur content of the used fuel or manipulating the combustion process in order to reduce NOx emissions. Secondary compliance techniques apply exhaust gas after treatment to lower SOx and NOx emissions levels. On top of these possibilities, the fuel choice can tremendously influence the exhaust emissions.

Currently the fuel price for fossil fuels is at a minimum; With 176\$ per tonne (BW380, 30.12.2015, [3]), the fuel is as cheap as it wasn't for 20 years. This situation of very cheap fuel and new legislations for ships to enter emission control areas lead to an unpredictable situation with respect of fuel choices. In the mid term future, about 60% of the ships will be propelled by classic fuels like residual fuels or some destillate fuels (Marine Gas Oil, Marine Diesel Oil). But an unknown number of ships might use exotic fuels. Depending on their price and availability, very exotic alternative fuels (for the rather conservativ shipping market) could be used in shipping – e.g. ethanol, methanol, LPG etc.



2 Goal of the FlexiFuel combustion project

A prediction of the future fuel alternative for the shipping business is not easily accomplished. Hence, engine manufacturers need to prepare their products for a variety of fuels. The question is which fuels possibly can be applied in the Diesel process. In order to investigate candidates for possible fuel alternatives, the experimental setup in Oberwinterthur had to be adapted to investigate the spray morphology or ignitability of fuels with different chemical and/or physical properties.

The goals of this project were therefore:

- the adaption of the Spray Combustion Chamber towards higher flexibility of the injection system
- to extend the application range of the measurement equipment (e.g. PDA for opaque fuels)
- to test a small range of fuels

Also in 2030, the major part of the world's cargo ships will be fuelled with conventional fuels [1]. In order to reduce their nitric oxide emissions (and probably others), also those "classic" fuels need to be understood better, to maintain or improve the engines efficiency while fulfilling the legislations. Therefore existing methods had to be adapted to deepen the understanding of classic fuels like residual or distillate fuels.

All over, the goal of the FlexiFuel project was to acquire fundamental understanding of the processes inside the engine and their dependence on fuel specification. Furthermore it remains to be clarified how the choice of injection parameters – including the layout of the injection systems key components – can be used, in order to minimize the impact of a change in fuel quality on the engines reliability and performance.

Obviously, the actions planned during the FlexiFuel project have high practical relevance for the further development of large, marine, two-stroke diesel engines. On the other hand demand the required investigations the application and further development of suitable diagnostic methods, as well as evaluation methods and simulation tools.

The goals of the current project also covered the following goals of the SFOE's energy research concept:

- System optimisation for a flexible application of different fuels
- System optimisation for the application of bio derived fuels
- Further development of test rigs for the validation of simulation models
- Improvement of simulation models and broadening of the knowledge on chemical and physical processes during combustion
- Strengthening the cooperation between industrial and university research, as well as the further development of the research competences

3 Concept – The Spray Combustion Chamber

The experiments presented in this work have been carried out in the so-called *Spray Combustion Chamber* [5]. This test rig consists of three main parts: Pressure vessels, which can be filled up to 35 MPa with N₂ (non-reactive cases), air (reactive cases), or some gas mixture (e.g. N₂, O₂ and CO₂ for simulating EGR-conditions). The second part is the so-called regenerator, where over a large surface the gas can be heated up before it flows over tilted inlet ports (generating strong swirl) into the SCC main body. This is a disk shaped constant-volume cell, representative of the dimensions of a large marine four-stroke or a medium-sized marine two-stroke diesel engine. The bore of the combustion chamber is 500 mm and its height is 150 mm. To cover most of the conditions relevant for large marine diesel engines, pressure, temperature and swirl velocity can be controlled almost fully independently by proper selection of the system's main parameters such as pressure in the vessels, temperature of the regenerator and blow-down time. Flow investigations were performed by means of LDV for demonstrating that the chamber fulfils the requirements not only regarding pressure and temperature ranges envisioned, but also in terms of swirl pattern at start of injection [6]. Before combustion, gas pressures up to 13 MPa can be achieved, with gas temperatures up to more than 900 K and swirl velocities of up to 40 m/s. The setup is designed for withstanding peak firing pressures of up to 20 MPa. Figure 2 shows the schematic overview of the SCC, also illustrating the window position and size in relation to the chamber dimensions.

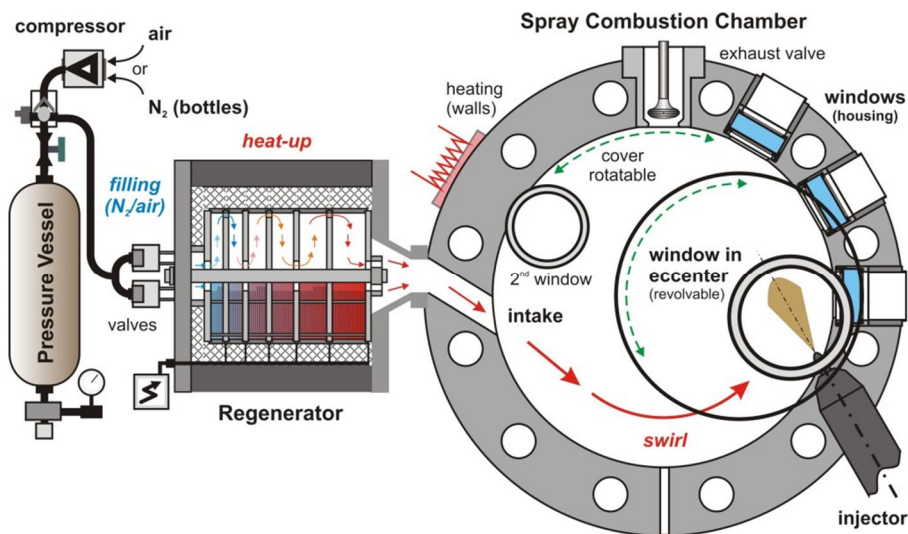


Figure 2: Schematic of the SCC

Optical access is provided by large sapphire windows (optical diameter 150 mm) mounted in eccentric revolvable window holders located in the rotatable covers. With specified resisting pressures up to 250 bar (incl. safety factor of 4) (and other advantageous properties (scratch and thermo-shock resistance, thermal conductivity)) they represent an optimum in maximum optical accessibility and applicability compared to producibility and cost. By means of proper selection of the mounting angle of the cover and/or the eccentric window holders, virtually the whole volume of the SCC can be made optically accessible. Additionally, there are three locations in the outer ring, giving access also perpendicular to the side windows for specific purposes (e.g. illumination, PDA-access etc.). Table 1 gives an overview of the key parameters of the SCC.



Bore	500 mm
Height	150 mm
Optical access	2 x 150 mm; 3 x 65 mm
T max before injection	>900 K
p max before injection	13 MPa
p max after combustion	20 MPa
Swirl velocity	Up to 40 m/s (@ r=200mm)

Table 1: Specification of the Spray Combustion Chamber

4 Methodology

4.1 Continuous usage of an established, unique test vehicle

After almost ten years, the SCC is still to be regarded as a unique experimental facility which not only allows the observation of the most important internal engine processes under relevant conditions: Due to the wide and flexible optical accessibility as well as the wide range of applicable conditions, the SCC also allows the quantitative analysis of spray morphology, ignition and combustion. The previously conducted experiments have indeed contributed a lot to a better understanding, already. But there are still a lot of unanswered questions, where the SCC provides the ideal base to answer them by means of specific tests. The proposed project is far also protecting previous investments in the construction and further development of this unique infrastructure. With regard to the international Wettbewerbsfähigkeit of the above-mentioned consortium Swiss research partners, the availability of such an instrument also represents a decisive advantage.

4.2 Investigation of the influence of non-conventional fuels

Beyond the investigations of a small number of representative fuels so far, further non-conventional fuels shall be looked at. The scope was to be both toward superior grade (in the marine sector not common) fuels, at best to model or synthetic fuels, as well as extended towards particular including those as extreme characteristics. Especially fuels with physical properties – such as density or viscosity – outside of the ISO standards or because of their different composition (examples: very high aromatic content, emulsions, specific additives) can be expected to change the behaviour of breakup and evaporation processes. The influence of biogenic fuels - either as a substitute fuel or in admixture with a base fuel with known behaviour – should be examined as well.

4.3 Consideration of future requirements for increased fuel flexibility

Large marine engines of the future will much more be forced to switch between different fuel types than they are now. Partly because increased regional regulations ask for the use of higher quality fuels, on the other hand large regional availability and price differentials might be attractive for ship owners to bunker different fuel qualities/types. Such switching between different fuels could therefore either be purely



changing the fuel supply or require switching between two different injection systems. Corresponding tests must therefore take both possibilities into account, which means that a wide range of future injection systems must be covered. In addition, it can be assumed that injection pressures in future engines will significantly be increased.

4.4 Extension of the test rig by developing and implementing suitable components and systems

The realization of the desired conditions in the chamber during the injection may require certain adjustments to the chamber geometry, especially if investigations under elevated injection pressures should prove necessary. The same applies to the influence of flow conditions in the combustion chamber (swirl intensity). Corresponding requirements were clarified by appropriate preliminary investigations in the first phase of the project.

5 Results

5.1 Injection process/ Dual-/Multi fuel systems

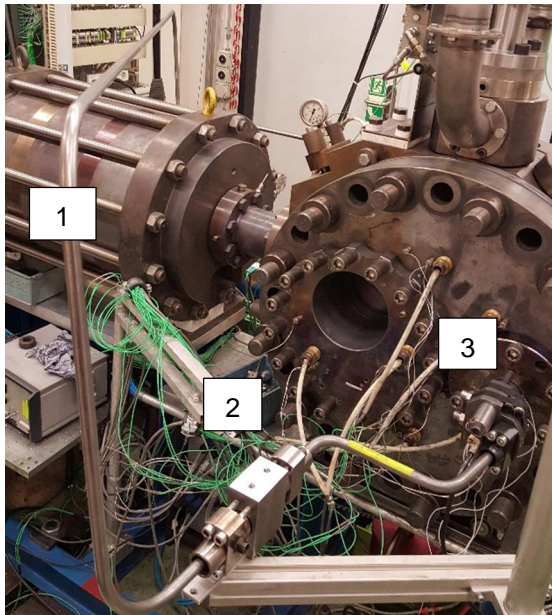


Figure 3 - L'Orange injection system:

1. High pressure piping
2. Adapter
3. L'Orange injector with needle lift and pressure before needle measurement

To increase the flexibility of the injection system and enable for time-controlled injection, four injectors from L'Orange have been acquired. These injectors belong to the new common rail system with solenoid actuation for constant injection pressure during the injection process. Their design allows the application of multiple injections. For large marine diesel engines this method is not investigated, yet. But a multiple injection strategy shows potential to offer additional parameters to control the injection process and therefore influence the combustion. This would allow for engines with higher flexibility. Such a system has already been introduced on small and mid-sized two stroke engines.

The new setup allows the SCC not only to investigate the classic – and worldwide proven – RT-flex system with a so-called injection control unit (ICU) [7], it enables a direct comparison with and the investigation of modern systems. The new setup was also necessary in order to support the development of smaller and mid-sized engines using the new injection system.

The SCC is now equipped with a highly flexible and adaptable injection system covering most of the demands of a test setup and allowing for the investigation of a variety of different engine types and sizes. The rather small and simple installation

helps therefore to increase the value of the installation and to maintain the status of the test rig as a highly flexible tool with a wide range of conditions and applicable techniques.

5.2 Droplet sizes and velocity

5.2.1 Further development measurement techniques

In close collaboration with ETH Zürich and EMPA Dübendorf, the Phase Doppler Anemometry (PDA) system was rebuilt and extended. In a first step the system was used to determine whether it was possible to measure droplet size and droplet velocity of opaque fuels. Therefore the system was set up in the laboratories of LAV at ETH in Zürich. Figure 4 shows the setup used in the laboratories of LAV; It consists of three major components: The sending optics which produce a measurement volume in the spray, receiving optics to detect the signals from droplets passing the measurement volume and to condition the signals before they're sent to the processor for determination of droplet size and velocity.



Figure 4: Left - Overview of PDA System. Right - Top view on the experimental setup with: (1) mono-disperse droplet generator, (2) front lens PDA transmitting optics, (3) PDA receiver

After years of inactivity, the PDA system (belonging to ETH Zürich) has been reactivated. Most of the components were in very good condition. However, the sending optics showed some traces of time. The argon-ion laser would have needed a complete overhaul, which included the acquisition of a new lasing tube. This would have almost been as expensive as replacing the whole laser system. Additionally, some parts of the carrier unit holding the beam separation optics, had been consumed over the years by other optical setups. Therefore the entire sending optics was rebuilt again from scratch. Based on the setup presented in [8] and according to the design of [9] new sending optics have been developed in collaboration with ETH and EMPA. They consist of two optically pumped semiconductor lasers emitting linearly polarized beams at 514.5 and 488 nm (OPSL; Coherent Genesis CX-Series SLM) which have been tailored to the needs of the PDA system. These two lasers are replacing the Ar⁺-laser from the old setup. The new laser system is more cost effective as the two individual laser sources consume significantly less electrical power than the old Ar⁺-laser. The two colours do not need to be extracted from one laser beam anymore, what reduces the alignment efforts, amount of optical components and it makes the system much less sensitive to temperature changes, compared to the earlier system [10] or its twin-system stationed in Loughborough described in [11] or [12].



The detector is a Dantec system consisting of a receiver (57X10) and an enhanced signal processor (58N10) including analysis software (SizeWare 2.3). The most important parameters of the laser, respectively the sending and receiving optics, are summarized in Table 1 and documented by Schneider [10].

Parameter	Unit	Main Flow Direction	Transversal Flow Direction
Wavelength	[nm]	514.5	488
Laser Power	[W]	0.02 - 4	0.02 - 2
Frequency Shift Bragg Cell	[MHz]	40	40
Polarization State	[-]	Linear	Linear
Focal Length Transmission Lens	[mm]	350	
Beam Separation	[mm]	45	
Fringe Spacing	[μm]	4.01	3.80
Number of Fringes	[-]	20	20
Measurement Volume Diameter	[μm]	80	80
Elevation Angle	[$^{\circ}$]	0	
Focal Length Receiving Lens	[mm]	310	
Scattering Angles	[$^{\circ}$]	70, 90, 105	

Table 2: Laser, transmission optics, measurement volume and receiving optics

5.2.2 Droplet Generation

Steady and reproducible droplet generation is the key to successfully investigate the behaviour of any droplet measurement technique with regard to its capabilities, features and specialities. An aerosol generator (Palas PLG 2010) capable to atomize HFO at elevated temperature level was used to investigate the smaller droplet diameters (up to 10 μm). The working principle is based on a Laskin nozzle, a compressed air nebulizer where the operating part is immersed in the liquid.

For validation measurements at larger droplet sizes and to further corroborate the results, investigations with a device able to generate droplets of one particular size were performed. For this purpose, a custom-made continuously operating monodisperse droplet generator with heating capabilities – as a prerequisite for the applicability of HFO – has been used.

5.2.3 Imaging System

The verification measurements of the droplet diameter have been performed by means of simultaneous shadow imaging. The background was illuminated by a xenon flash light in combination with a diffusing plate to create a homogeneous background with equally distributed intensity (see Figure 1, right). The images were recorded using a 12bit CCD Camera (resolution 1280 x 1024 pixels) with an exposure time of 2.5 μs at a frame rate of 15 fps.

Investigations assessing the feasibility and applicability of the PDA technique to measure droplet sizes and velocities in HFO fuel sprays at relevant conditions were conducted. In general, the scattering amplitude of a single droplet in a laser beam depends on the refractive index, the wavelength of the laser, the droplet diameter and the scattering angle. Therefore, the refractive index of droplets of the fuels under consideration had to be determined, including its dependence on operation parameters. This

also involves the identification of the dominant scattering mode, which is based on the Mie scattering calculations and the assessment of the phase difference - diameter relationship.

5.2.4 Determination of the complex refractive index

Besides the scattering angle θ , the relative refractive index \underline{m} is the most important parameter in a PDA measurement setup – apart from more system-related parameters like wavelengths, beam separation and elevation angles. The relative refractive index \underline{m} is defined as

$$\underline{m} = \frac{n_d}{n_m}$$

with n_d as the complex refractive index of the droplet and n_m of the surrounding media. It influences the measured droplet size distribution profoundly as it determines the relative intensities of the different light scattering modes and thereby the phase difference - droplet size relation for a given scattering angle. The complex refractive index defined as

$$\underline{n} = n - i\kappa$$

where the real part $n = \sqrt{\epsilon_r \mu_r}$ describes refraction and the imaginary part $\kappa = \alpha\lambda/4\pi$ is defined as the extinction coefficient κ in dependency of the absorption coefficient α and the wavelength λ . Media with strong light absorption behaviour cannot be characterized simply by the refractive index n . In this case, the complex refractive index with the extinction coefficient $\kappa > 0$ as the imaginary part needs to be taken into account.

If the scattered light collected by the PDA receiver contains a substantial amount of refracted light, the determination of the relative refractive index must be considered indispensable for valid measurements. In contrast, highly absorbing media allow exploiting reflected light for the phase difference - diameter relationship as almost no refracted light is able to pass through the opaque droplets. This leads to the major advantage that the relative refractive index \underline{m} does not depend on the real part n of the complex refractive index. Due to the fact that both mentioned scattering modes have been examined, the measurement of the refractive index n was absolutely essential for the refraction case.

Ellipsometry is a well established experimental method for measuring the optical constants (refraction index, extinction coefficient). The technique is based on the effect that polarization changes if light is interacting (e.g. reflected or transmitted) with a media surface. A simple Cauchy model has been fitted with the measured data to obtain the refractive index and the extinction coefficient was identified via the Urbach model.

To validate the measurements of the refractive index, critical angle refractometry experiments have been performed as the measurement technique is able to determine refractive indices of transparent as well as absorbing media. On a digital refractometer, the real part n of the complex refractive index \underline{n}_d could be obtained at the wavelength of 589 nm (Na_D-line). The device is equipped with a built-in Peltier element allowing investigations on the temperature dependency of the refractive index (T_{\max} 60°C).

Investigations have been performed at ambient pressure and temperature conditions using both spectroscopic ellipsometry and refractometry. Furthermore, the heating capability of the refractometer has been exploited for measurements of the temperature influence on n . Subsequently, the obtained values have been extrapolated to the temperature level at which HFO is injected into the combustion chamber. Experiments for different fuel types and water as reference media were intended. However, it



was not possible to determine the complex refractive index of the low quality HFO due to certain limitations (e.g. measurement range of the refractometer) of the available test equipment.

The results of the refractometer measurements for both, LFO and HFO, showed a decrease of the refractive index with increasing temperature and are in good accordance with earlier measurements by Astachow et al. (1993) and Dombrovsky et al. (2003). For the present investigation, the refractive index was extrapolated to the desired temperature level of about 100°C.

The assessment of the complex refractive index with the ellipsometer offered the possibility to measure in the whole visible spectra and allowed to simultaneously capture the extinction coefficient κ . Moreover, the values obtained by the refractometer could be compared with the results of the experiments based on spectroscopic ellipsometry. In Figure 5 (left), the refractive indices for HFO, LFO and water over a spectrum of 400 to 1000 nm are shown. The numeric values highlighted at 514.5 nm (emitting wavelength of the laser utilized for size measurement) are in very good agreement with the values obtained by refractometry at 589 nm.

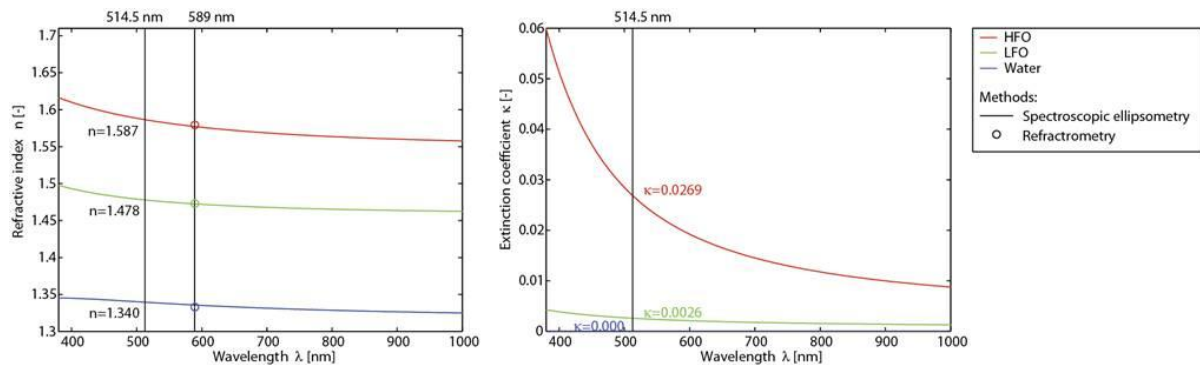


Figure 5: Refractive index determination: Left - comparison of the refractive index obtained by refractometer and spectroscopic ellipsometry; Right - extinction coefficient over wavelength.

5.2.5 Marine Diesel Fuel Droplet Characterization by Means of PDA

Preliminary investigations were performed by [13] in order to evaluate the light scattering behaviour in regard to the corresponding LFO/HFO fuels. Single droplet Mie scattering characteristics show a significant difference for transparent and opaque media, especially for bigger droplet diameters ($> 25 \mu\text{m}$). For LFO, the first order refraction and the Mie scattering correlate well showing almost the same intensity levels for both, perpendicular and parallel polarization. Furthermore, for parallel polarization at the Brewster angle only refracted light is present as the reflective part vanishes. Therefore, this is a well-known option for PDA measurements in transparent media as seen in earlier investigations (e.g. Wigley, 1998). On the contrary, the Mie scattering intensity for HFO is very close to the reflective part of geometrical orders for both polarizations. For parallel polarized light generally lower Mie scattering intensity is present – compared to perpendicular polarization – with the absolute minimum at the Brewster angle. Thus, for HFO, a reflective mode in combination with perpendicular polarization should be preferred.

Based on these findings, investigations with regard to the phased difference - diameter relationship were performed to determine possible configurations for the scattering angle where the Mie scattering

corresponds well to geometrical order as the PDA-processor uses a constant factor between phase difference and diameter to define the droplet size.

Due to the similarity of the fuels, the same approach of using parallel polarization and a scattering angle of 70° (Brewster) as commonly used for PDA measurements in Diesel fuel sprays 4 has been applied for the transparent LFO investigations. The phase difference - diameter relationship can be well described by a single phase difference - diameter factor over a wide range of droplet sizes. Since the reflective part of the scattered light is completely missing, this specific configuration would also be favourable for HFO measurements if the intensity of the refracted light passing through the fuel droplet would be sufficiently high. However, as can be seen in Figure 6 (left), which shows the phase difference - diameter relationship determined with light scattering analysis for parallel polarized light collected at 70° scattering angle, this not applicable for the complete size range of interest: The first section from 0 to $5\ \mu\text{m}$ droplet diameter demonstrates good agreement with the refractive part of the geometrical orders; the third section from $\approx 12\ \mu\text{m}$ on is almost in perfect agreement with the reflective part. However, due to the increasing absorption of the light in the drop size range between 5 and $12\ \mu\text{m}$, the transition from dominantly refracted to mainly reflected light results in high uncertainty concerning the relation between phase difference and droplet diameters.

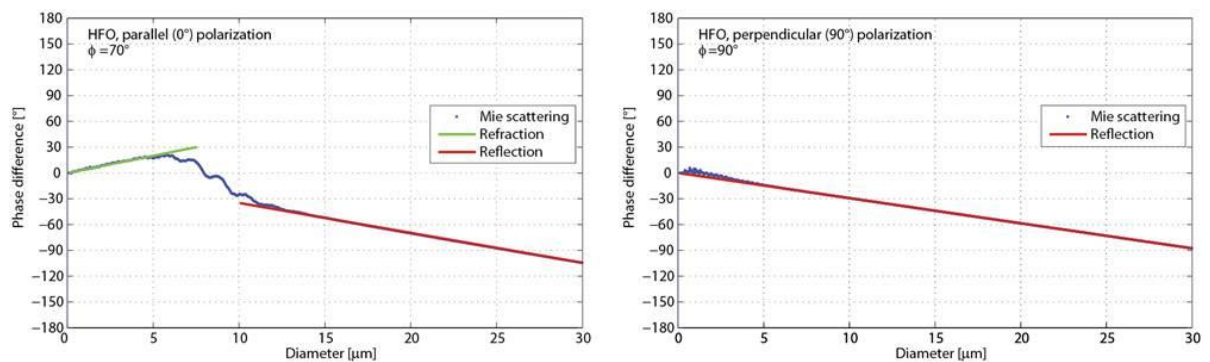


Figure 6: Phase difference - diameter relationship of HFO droplets at 70° parallel

A further promising PDA configuration for HFO spray investigations with a scattering angle of 90° in combination with perpendicular polarized light has been identified by corresponding Mie scattering / geometric optics calculations. The resulting phase difference - diameter relationship is presented in Figure 6 (right). The comparison of the phase differences for very small droplets indicates that a non-negligible amount of refracted light is still present in this range and the corresponding sizes are generally underestimated. However, for droplet diameters above $5\ \mu\text{m}$ quite pure reflected light is collected by the receiver. For droplets larger than $\approx 10\ \mu\text{m}$, the phase difference - diameter relationship is close to perfect. Another viable scattering angle would be 105° with the same polarization state as at 90° , where reflection is the only dominant mode based on geometrical optics calculations. Therefore, the same tendencies as for 90° , are present and the differences in the resulting phase difference - diameter plot are very small. The scattered light intensity is slightly lower, but the relative error between the phase differences of Mie scattering and reflection at $\approx 5\ \mu\text{m}$ is somewhat better.

To validate and assess the evaluated scattering angles and corresponding polarization states above, PDA measurements with both an aerosol generator (droplets up to diameters of $10\ \mu\text{m}$) and a monodisperse droplet generator in conjunction with the imaging system have been performed. Due to the inability of the monodisperse droplet generator to create droplets smaller than $60\ \mu\text{m}$ diameter, the aerosol generator is used to gain information with regard to the smaller droplets regimes. Figure 7 shows the HFO droplet size distribution measured for refracted light at 70° scattering angle (parallel polarized,



first order refraction) as well as for reflected light at 105° scattering angle (perpendicular polarized, reflected light). Both distributions were derived from 20'000 validated samples. The different results in the lower droplet diameter regime (< 5 μm) illustrate qualitatively the limitations of the PDA system concerning the correct acquisition of small HFO droplets due to arising uncertainty in the phase difference - diameter relationship. As shown in Figure 6, refracted light dominates the phase difference - diameter relationship for very small droplet diameters below 5 μm and reflected light for droplets above 10 μm, which is causing those irresolvable ambiguities in the transition zone in between. This non-linear and discontinuous phase difference - diameter relationship leads to the rejection of such droplets as the processor analysis is based on a constant correlation factor between phase difference and diameter for the size determination.

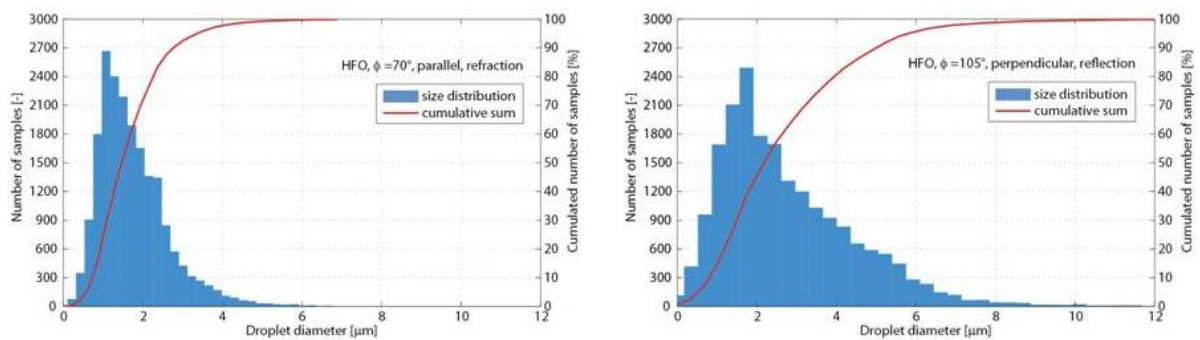


Figure 7: Droplet size distribution of HFO ($m = 1.538-0.269i$) under the Brewster angle (left) and a scattering angle of 105° (right)

As described above, only configurations with 90° or 105° scattering angle at perpendicular polarization yield consistent results over a wide range of droplet sizes. However, due to considerations related to the optical accessibility of the Spray Combustion Chamber, only the 90° scattering angle PDA setup is applicable. Hence, corresponding validation measurements using the mono-disperse droplet generator have been performed for HFO. In addition, LFO measurements with a scattering angle of 70° and parallel polarization have been conducted. The simultaneously recorded shadow images of the droplet chain emerging from the generator have been post-processed to gain validation data for LFO/HFO droplet size measurements with the PDA technique. By means of circular Hough transformation (see Atherton et al., 1999), an automated search for the size classification of the droplets could be provided. Figure 8 shows one exemplary HFO droplet size distribution measured by PDA (left) and the corresponding result based on the analysis of the camera images (right). Furthermore, the correlation between PDA results and image analysis in the 100 to 180 μm range for both, LFO and HFO droplet size measurements is displayed (middle).

The droplet sizes measured by means of PDA are in good agreement with the droplet size classification on the basis of the shadow imaging recordings. This clearly indicates the capability of measuring heavy fuel oil droplets with PDA for the configuration and conditions relevant to large marine Diesel injection and combustion systems.

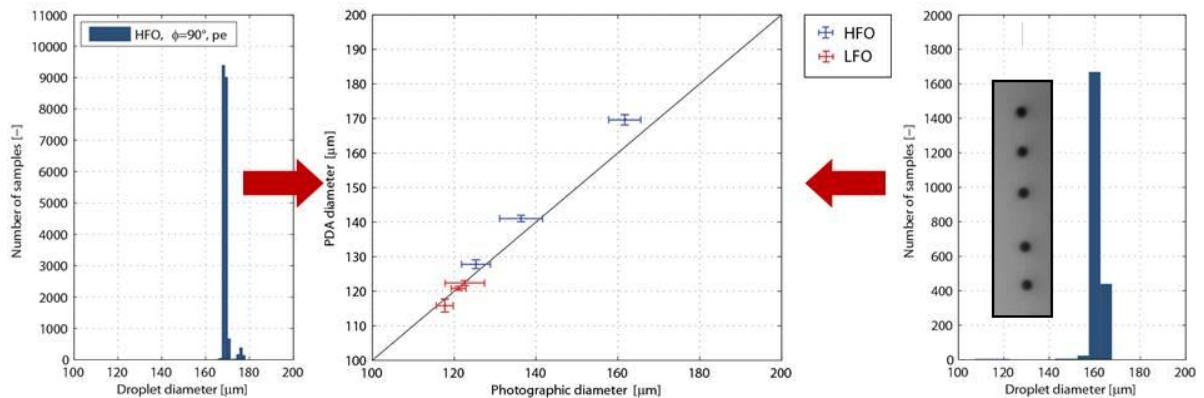


Figure 8: Validation experiments with a mono-disperse droplet generator for HFO and LFO measurements. One exemplary HFO experiment with PDA measurements (left) and simultaneously acquired shadow imaging recordings as well as size distribution (right) is shown

5.2.6 Experimental investigations under engine relevant conditions

Light fuel oil

With the new setup, PDA measurements have been conducted in the SCC. Under temperature and pressure conditions, comparable to those in an engine, droplet sizes and velocities have been measured in the spray of a single hole nozzle. The results contribute to a better understanding of the spray breakup for such large engines and deliver valuable input for the validation of spray models and calculations.

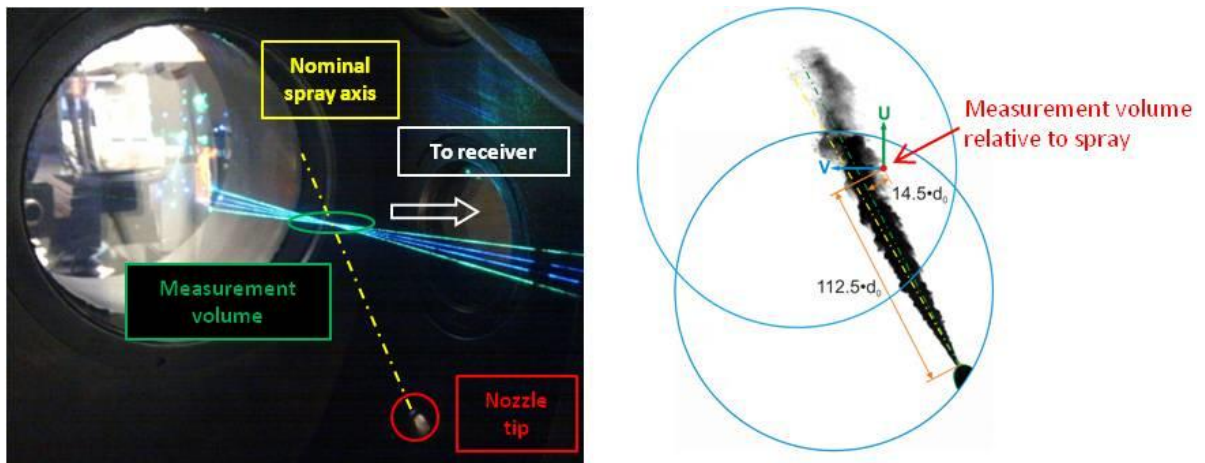


Figure 9: PDA Application at the Spray Combustion Chamber (left) and schematic illustration of the measurement location within the spray plume, indicating the measured velocity components (right).

The experiments were performed under both evaporating (but non reactive: nitrogen as process gas) and non evaporating conditions. The evaporative case was at a pressure of 90 bar and a temperature of 900 K which results in a density of 33.8 kg/m³ and corresponds to the engine conditions of about 50%



load. The non evaporating cases were at 40 bar and 400 K, which result in a density of about 34.8 kg/m^3 . The comparison of the measurements under these two conditions allows an estimation of the evaporation process on the fuel droplets. The injected fuel spray (rail pressure 1000 bar) originates from a single hole injector with a co-axial orifice. Figure 9 (left) gives an impression of the nozzle tip location and the optical accessibility with regard to the laser beams forming the measurement volume, respectively the location of the receiver acquiring the scattered light. The reference measurement position in the spray is located at a distance $112.5 \cdot d_0$ downstream and with regard to the sprays centreline at $14.5 \cdot d_0$ of its radial periphery (Figure 9 right). To investigate the droplet size distribution in axial direction, measurements were conducted at three different distances from the nominal spray axis. The experiments of this first series were performed with light fuel oil (LFO).

If the signal recorded by the PDA receiver is looked at over the whole injection process, it shows low intensity levels during the injection. This is an indication for the very dense nature of the investigated spray at the measured locations and hence, only low validation rates could be achieved due to the obscuration of the input beams and the signal path to the receiver. Therefore, an adequate number of measurements had to be performed (typically between 50 up to 100 repetitions) to gain sufficient information for a significant result. The consumption of about 2000 kg of N_2 was the price of these investigations. In order to validate the results, not only 2D-PDA measurements have been conducted but also 1D-PDA as well as 2D-LDA (Laser Doppler Anemometry) experiments with increased data and validation rate. These experiments were also included in the analysis to enhance the significance of the results.

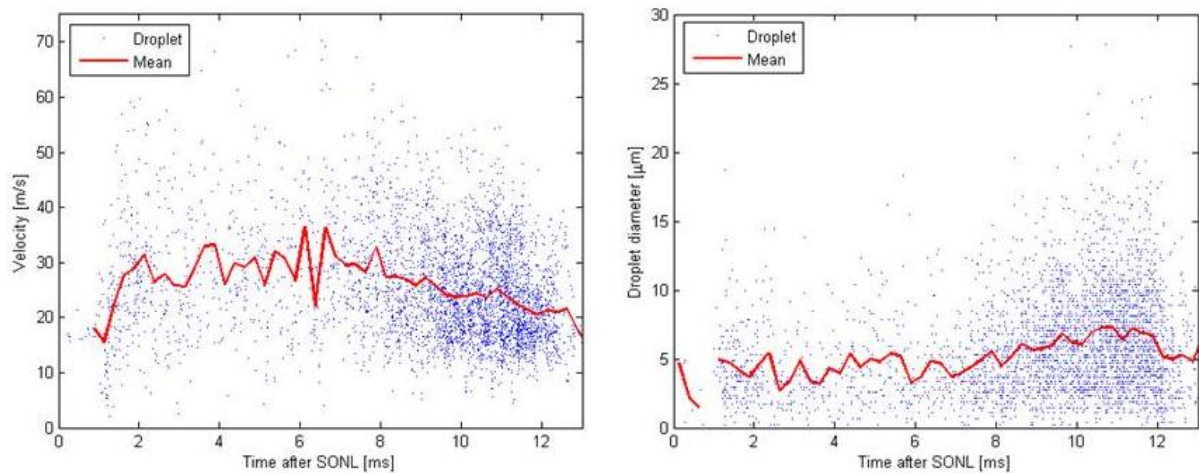


Figure 10: Droplet velocity (left) and droplet size (right) of LFO spray injected at 90 bar and 900 K chamber condition.

In Figure 10 the temporal evolution of droplet velocity (left) and droplet size (right) of the injected LFO sprays are shown. Each measured droplet is indicated (blue) and the mean value (red) per evaluated time bin ($250 \mu\text{s}$) can be seen in the graph. Moreover, the closing of the needle is indicated to highlight the spray boundary conditions. The droplet velocities show the absolute velocity magnitude in the spray derived from the two simultaneously measured velocity components U and V (compare Figure 9, right).

At the start of injection the velocities of the measured droplets increase due to the still not fully established and therefore increasing spray momentum. During the subsequent main injection phase, the droplet velocities show a mean value of about 30 m/s with peaks up to 75 m/s. This indicates a high degree of interaction between the spray and the surrounding gas. Towards the end of injection the

droplet velocities slow down due to the decrease of the momentum in the spray, as the injection pressure starts to decrease. In this stage a higher data rate was obtained as the main spray was over and the optically less dense spray increased the probability for a droplet to be measured.

On the right image in Figure 10 the corresponding droplet sizes can be seen. For the period of the main injection a mean diameter (D_{10}) of about 14-18 μm is observed while the largest droplets which could be measured are about 25 μm . Towards the end of injection, the size of the droplets is slightly increasing, which is a result of the reduced spray momentum due to the decreasing injection pressure.

In Figure 11 the averaged droplet velocities and diameters for three radial positions (14.5, 12 and 9.7· d_0) are plotted as a function of time after start of needle lift (SONL). The droplet velocities measured for the reference case (red curve, $R=14.5\cdot d_0$) are clearly the slowest. Towards the centre of the spray, the averaged droplet velocity increases. Interesting is the fact that after end of injection (around 10 ms) the droplets have about the same velocity. This is when the spray no longer dominates the velocities, and the droplets are carried away by the strong gas swirl flow.

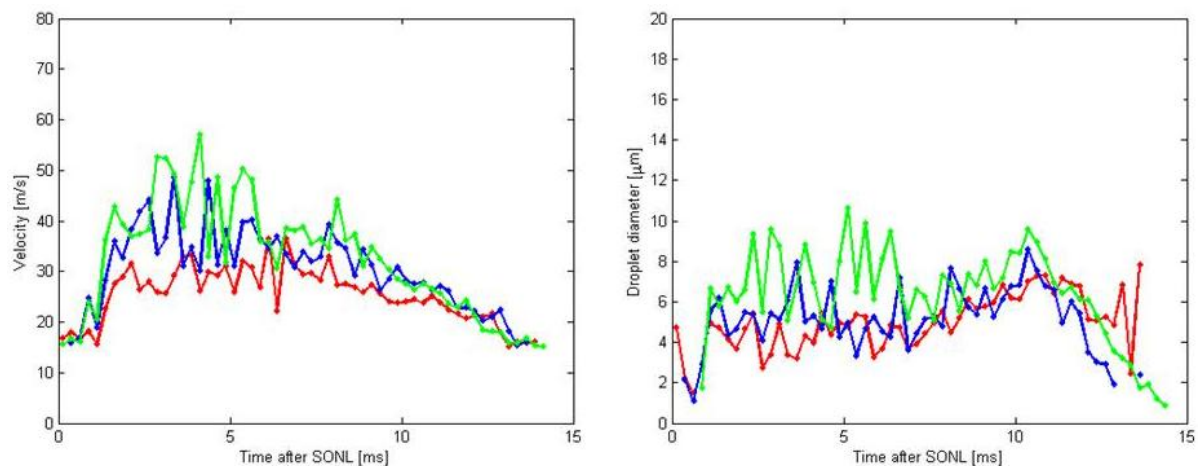


Figure 11: Mean droplet velocity (left) and droplet size (right) in a radial cut of the LFO spray at 90 bar and 900 K chamber condition.

The corresponding droplet sizes – right hand side of Figure 11 – slightly indicate the influence of the evaporation at the spray boundary. A reduction of the measured mean droplet diameter can be observed when the droplets on the inside (green curve, $R=9.7\cdot d_0$) are compared to the outside of the spray plume.

Heavy fuel oil

For the first time the droplet sizes and velocities of a heavy fuel oil spray have been investigated under engine relevant conditions. Figure 12 shows the temporal evolution of droplet velocity (left) and droplet size (right) in case of HFO sprayed into the high pressure, high temperature environment of the SCC. For the measurement series standard conditions have been applied (90 bar, 900 K) to allow a comparison of the results over the whole measurement campaigns conducted so far. For the visualisation each individual droplet is plotted (blue) over the time of its arrival in the measurement volume. To allow a better perception of the data, the average per evaluated time bin – 250 μs – is shown in red. In order to compare the data with the injection timing and to highlight the spray boundary conditions, the moment when the needle was closed is indicated with a broken black line.

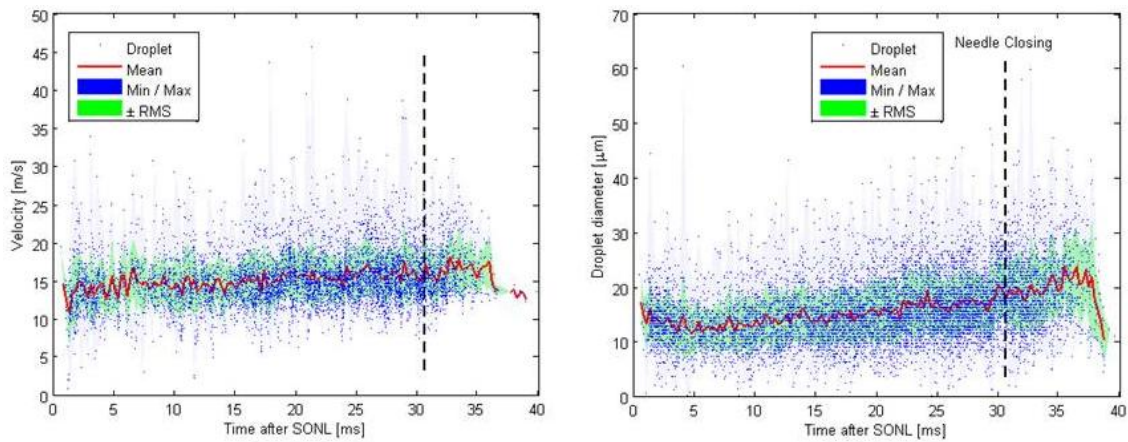


Figure 12: Droplet velocity (left) and droplet size (right) at 90 bar and 900 K chamber condition

The droplet velocities show the absolute velocity magnitude in the spray derived from the two simultaneously measured velocity components.

In the very initial stage (up to 2 ms after start of needle lift), the velocity at the spray tip is decreased due to not yet fully established momentum of the injection. During the subsequent main injection phase, the resulting droplet velocities show a mean value of about 15 to 17 m/s with peaks up to 50 m/s). This indicates a high degree of interaction between the spray and the surrounding gas yielding highly turbulent recirculation zones in this region of the spray. Moreover, the spray droplet velocity is influenced by the high swirl flow acting on the spray (ca. 13 m/s). At the end of the injection, it can be recognized that the droplets are only transported further by this flow.

The droplet sizes of the injected HFO spray show diameters up to 60 μm . At the beginning of the injection, the measured droplet sizes tend to decrease slightly in correspondence to the droplet velocities due to still increasing injection pressure in this very initial phase (2 ms after start of needle lift). For the period of the main injection, a mean diameter of about 14-18 μm is observed. Towards the end of injection, the size of the droplets measured is increasing again, which can be attributed to the reduced momentum of the spray as a consequence of the decreasing injection pressure after the injector needle has closed.

Comparison between LFO and HFO

To further assess the measurements performed at the HFO spray, a comparison with experiments at the corresponding LFO spray are presented in Figure 13. In particular, the difference of the fuel quality and its influence on the spray are discussed. The left side of Figure 13 shows of the normalized velocity distributions of the two fuels. The velocities observed with LFO are clearly higher and cover a larger range than those measured at the HFO spray. This unequal spread in the distribution of the velocities can be seen as an indication of the different nature of the two investigated fuels. The physical properties of LFO and HFO (especially with regard to difference of density and kinematic viscosity) have a significant impact on their atomization and subsequent evaporation behaviour. Nevertheless, a clear peak around 16 m/s in both velocity distributions can be recognized as most of the droplets tend to follow the high swirl flow in the chamber regardless of the fuel properties.

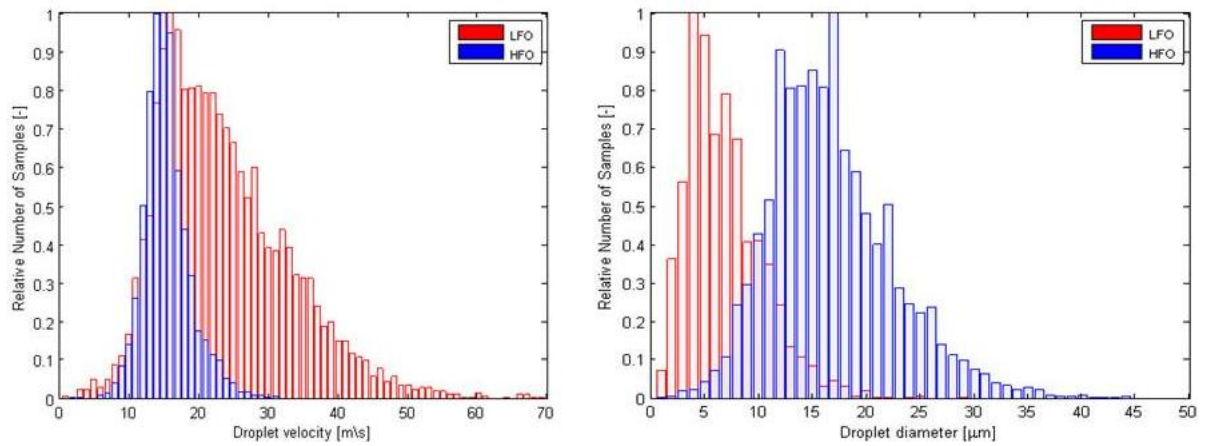


Figure 13: Droplet velocity and size distribution in the LFO (red) and HFO (blue) spray at 90 bar/900 K

The droplet diameter distribution is shown on the right graph of Figure 13. It can be readily seen that the droplet diameters of the HFO spray pile around a diameter of 16 μm while the peak in the droplet distribution of the LFO spray can be found at roughly 5 μm. Furthermore, a distinctly wider droplet size distribution is observed in the injected HFO spray with diameters reaching up to 50 μm whereas in the low viscosity LFO spray a maximum diameter at about 30 μm can be recognized. The higher viscosity and density of the HFO droplets lead to a clear difference in the droplet breakup and the following evaporation process. Besides the fluid properties, the significant lower content of low-boiling compounds in the HFO influences the evaporation of the droplets recognizably.



5.3 Ignition and Combustion

5.3.1 Further development Test rig - Adaption of the media separator

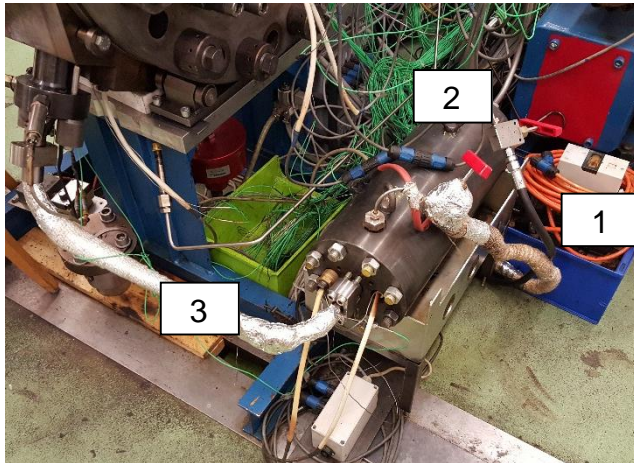


Figure 14: Media separator installed at the SCC with:

1. Feed pump
2. Media separator
3. Heated high pressure pipe

Preliminary measurements with the so-called media separator (MED) [8] showed a good general performance of this new tool. It allows a comparatively fast change of the fuel, provides a comparable injection pressure and injection profile as with the classic system and is relatively easy to clean. The MED was further improved with new drillings which allow a better flushing of the system, which considerably reduces the air pockets and therefore improves the performance of the setup. Additionally a new sealing concept was discussed with "Freudenberg Sealing Technologies". The additional sealing should further extend the number of injections per filling and therefore reduce the efforts. Especially when applying low viscosity fuels, the amount lost due to leakage is expected to be significantly reduced.

5.3.2 Ignition and Combustion by means of Spectroscopy

For three different fuels a series of spectroscopic investigations has been performed. The results of these studies will be shown in a journal publication by Mr. Beat von Rotz as a part of his PhD study. To guarantee the novelty of his findings a publication of these results will therefore be postponed to a later report. Instead a first investigation on three different marine diesel fuels is presented. The fuels which have been applied are the standard LFO which has already been investigated during the PDA measurements, a standard HFO, which has also been used in the SCC for and a rather poor quality HFO. These investigations shall verify the applicability of the SCC as a reference experiment for the examination of marine diesel fuels and have been presented in the SAE Fuel and Lubrication Conference in Birmingham:

Two optical measurement techniques were used to complement the findings made on the basis of rate of heat release analysis. A combination of the shadow imaging technique with the OH*-chemiluminescence method was applied to investigate spray tip penetration, ignition delay, ignition location, flame lift off as well as flame development of the heavy fuels in comparison with a light fuel oil.

The investigations presented in this work have been carried out at conditions representative of the operation of modern large two-stroke marine diesel engines. Gas pressure at the start of needle lift was set to about 9 MPa and gas temperature to around 900 K, resulting in a gas density of roughly 35 kg/m³, which corresponds to an engine load of about 50%. In this work, three different fuels have been investigated: A light fuel oil was applied as the reference fuel. Two different heavy fuel oil qualities have



been selected with similar values for density, heating values but with slightly different calculated carbon aromaticity index (CCAI) and with the viscosity of the second variant (HFO2) twice as high as for the first variant (HFO1). An overview of the fuel properties as well as the injection and thermodynamic conditions is given in Table 3.

Property	Unit	LFO	HFO1	HFO2
Gas pressure (SONL)	[MPa]	8.96	9.18	9.30
Gas temperature (SONL)	[K]	913,0	909,0	919,0
Gas density (SONL)	[kg/m ³]	34,2	35,2	35,2
Rail pressure	[MPa]	50	50	50
Fuel density @ 15°C	[kg/m ³]	851.3	989,7	994
Heating value	[MJ/kg]	42.47	40.41	40.53
Viscosity @ 50°C (ISO 3104)	[mm ² /s]	2.8	365	864
Cetan index (ISO 5165)	[-]	57.5	-	-
CCAI	[-]	-	851,6	847
Nozzle hole diameter	[mm]	0.875	0.875	0.875
Injected mass	[g]	4.2	7.3	7.2
Injection duration	[ms]	42	58	58

Table 3: Chamber conditions and fuel properties

For each investigated point at least ten experiments have been carried out (except for the case with HFO2, where due to technical reasons only 5 experiments have been performed). From each experiment the images have been evaluated individually and the resulting curves have then been averaged.

For these investigations, the rail pressure was set to 40 MPa, which after amplification in the media separator resulted in a pressure differential across the injector ($p_{\text{before needle}} - p_{\text{gas}}$) between 40 and 60 MPa. The injector is a serial injector with a tailor made nozzle tip, having a single, coaxial nozzle hole with a diameter of 0.875 mm. The injector temperature has been set to 100°C for all cases. Figure 15 shows the traces of needle lift and pressure in the injector (i.e. before the needle) for the three fuel types. Even though the three fuels cover a very broad range in viscosity, the system behaviour is largely similar, thus demonstrating a high degree of repeatability, which must be seen as prerequisite for the comparability of the results obtained.

For all cases, the pressure before the needle increases until the needle opens at about 38 MPa and the fuel flows into the nozzle tip. During this phase, the pressure slightly decreases due to the fuel exiting the injector's main body. The needle shows the same velocity during needle lift for all fuels and the pressure trace is very similar after the needle is fully opened and over the rest of the injection process.

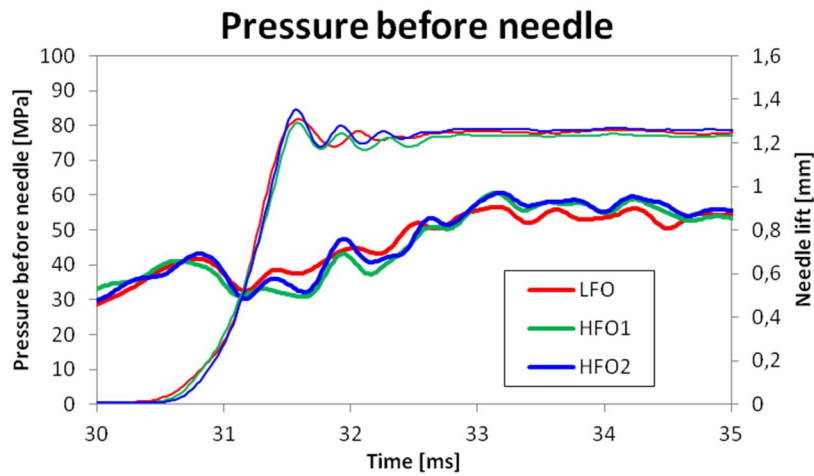


Figure 15 – Pressure and needle lift traces for LFO and HFO1&2

As already shown in [14], the ignition delay for LFO is around 0.6 ms. In Figure 16 the ignition delay for the three fuels is plotted over gas temperature during start of needle lift. The small points represent individual measurements whereas the larger markers are the average values of these individual results. The horizontal error bars represent the accuracy range of the temperature measurement, due to the limited precision of the applied thermocouples (type K), which is around $\pm 1\%$. The vertical error bars indicate the standard deviation of the ignition delay, which was measured with the help of the OH*-probe read out with a frequency of 500 kHz. As can be seen, the ignition delay for HFO2 is about twice as long as for LFO and the HFO1 takes almost 2.5 times the LFO ignition delay to ignite.

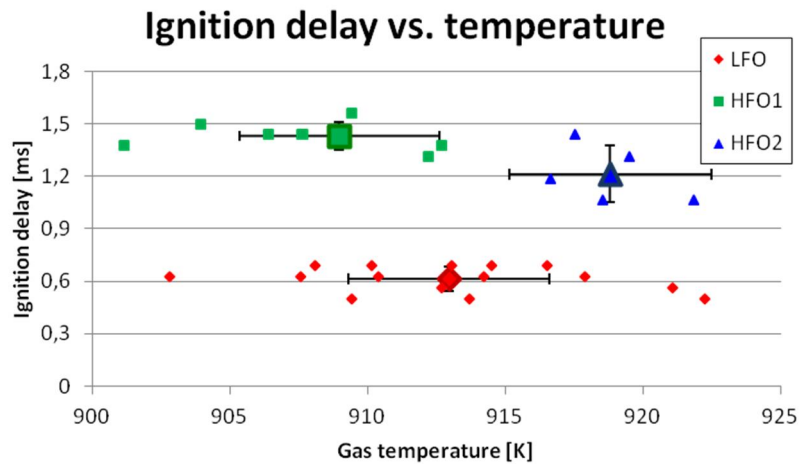


Figure 16 – Ignition delay for LFO, HFO1&2

This behaviour can be attributed to a variety of reasons, mostly related to one of the two phases of the ignition delay: If we assume that the chemical ignition delay is largely similar (if not constant) for all fuels, then the overall ignition delay is increased due to the physical ignition delay only. This phase is mainly governed by the atomisation and evaporation of the fuel, followed and accompanied by macro- as well as micro-scale transport mechanisms.

5.4 In-nozzle flow (Mie-scattering)

The diesel combustion process is strongly dependent on the rate of introduction of fuel and hence the quality of the atomization process, which in turn is significantly influenced by effects caused by the geometry of the fuel injection equipment itself as well as the potential occurrence of cavitation. In particular, the injector geometry of large marine two-stroke diesel engines differs substantially from the configurations used in most other diesel engine applications, as the injector orifices are distributed in a highly non-symmetric fashion. In order to simulate, respectively experimentally assess the impact of key features of such orifice arrangements on spray morphology, a generic nozzle design has been introduced in [17]. This specimen consists of an elongated tip with two orifices: The first one for producing the spray to be observed, the second one significantly far downstream of the first and with a diameter corresponding to the area of the remaining four orifices in a typical production injector, in order to simulate the same flow behaviour up to of the spray orifice. It was extended for the purpose of the present study by adding an insert, thus mimicking the flow conditions inside more recent injector designs.

Figure 18 explains the injector design presented in the first measurement series [17], with the fuel exiting the observed orifice (diameter d) while the fuel amount of another four orifices is bypassed through an additional orifice with diameter D whereas the area of the bypass-orifice is four times the area of the observed (and partially bypassed) orifice.

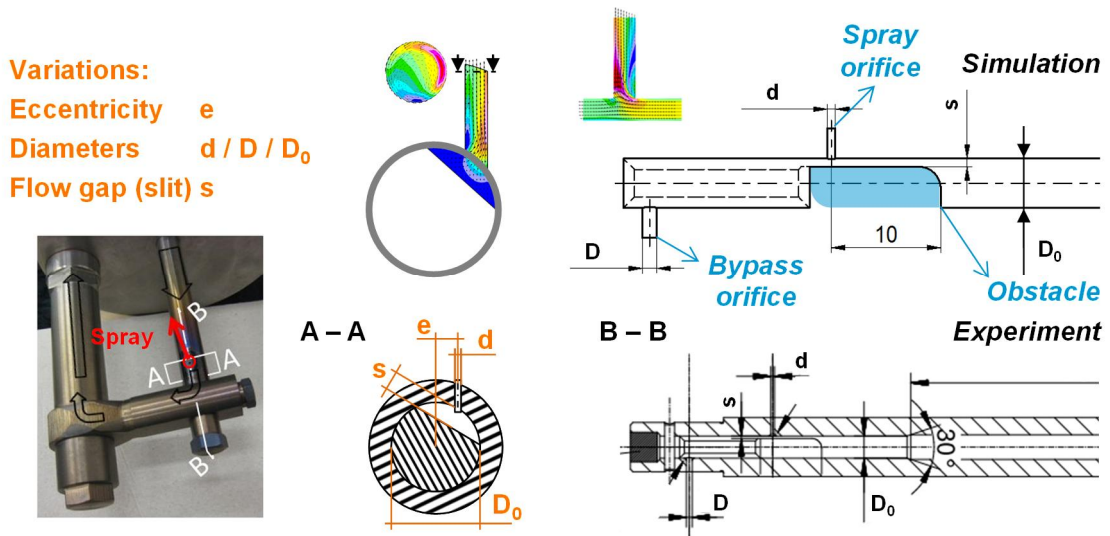


Figure 18: Schematic overview on generic nozzle design features, simulating the conditions of a single orifice within a serial injector

The generic nozzle design has been extended by adding an insert in the nozzle bore. This introduced a channel of height s underneath the orifice as can occur in more recent injector designs [18]. Figure 18 also shows the flow volume used for the simulations in comparison to the drawings of the experimental setup. Cut A-A explains the tilt of the channel in case of eccentricity. This was made to ensure a constant channel height. The channel was tilted such that the crossing point between the surface of the nozzle bore and axis of the orifice was located in the middle of the channel.

The geometric features of those five configurations – one reference geometry and four variations – are listed in Table 4: The injector configuration 2 (highlighted in blue) represents the reference injector while the four remaining configurations are the variations (highlighted in orange) in the nozzle eccentricity, channel height, nozzle bypass and turbulence generation. They are the configurations number 1, 4, 15 and 34, respectively, the apparently random numbers labelling the different injector configurations arise from a pre-selection of a large number of injector layouts. The four variations presented here were chosen to represent a balanced mixture of academic interest (#15 without bypass and #34 the swirl chamber) and industrial applications (#1 thin flow channel as can occur in more recent injector designs or #4 with eccentricity in combination with such thin channel). It is worthwhile noting that eccentricity is a characteristic feature of large two-stroke diesel injectors ([19], [20]).

Nozzle name	Nozzle number	d	e	s	D
[-]	[-]	[mm]	[%]	[mm]	[mm]
Reference	2	0.75	0	0.75	1.3
Eccentric	4	0.75	0.8	0.75	1.3
Thin channel	1	0.75	0	0.50	1.3
Without bypass	15	0.75	0	0.75	-
Swirl Chamber	34	0.75	0	0.75	0.5

Table 4: Injector configurations considered. Blue: reference injector. Variations are in orange: Introduction of eccentricity e , reduction of channel height s , comparison with single-hole nozzle and introduction of swirl.

Figure 19 shows the main elements of the generic injector design hardware for the particular configuration number 34, which involves a swirl-generation chamber underneath the orifice. The insert is fixed with a screw such that the swirl chamber is located in axis-symmetric position relative to the orifice.

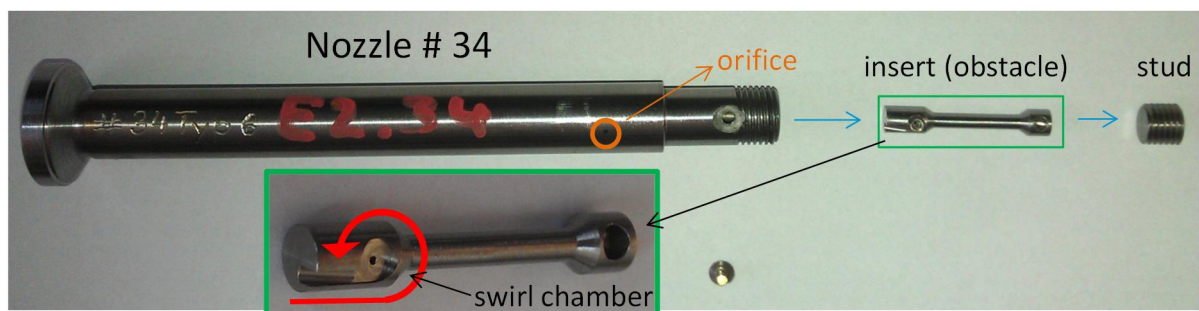


Figure 19: Nozzle configuration 34 with the insert to position the swirl chamber under the orifice.

For eccentric orifices, the generation of a swirling flow inside the orifice seems to contribute to clearly wider spray angles and sprays from such orifices are moreover characterised by non-negligible deflection from their theoretical axis. It could also be shown that it is essential to properly account for the actual flow conditions inside the injector, as single-spray tests neglecting the flow through the other orifices of a multi-hole injector yielded distinctly different spray behaviour, which would lead to erroneous conclusions when applied the results as is to multi-orifice configurations.



The five nozzle-hole configurations listed in Table 4 and discussed earlier have been tested under non-evaporating, no-swirl conditions. The gas pressure was set to 4 MPa and 400 K resulting in a gas density of about 33 kg/m^3 , rail pressure was set to 80 MPa: The conditions in the SCC are hence largely similar to those in an engine running at medium load, except for swirl and temperature.

For the comparison of the different cases, the spray during the steady injection period has been analysed. Note that this approach was first verified and applied for investigating sprays from traditional injectors without insert and the results of those earlier investigations [17] serve as additional references in the discussion below. For the analysis of the results, the individual images acquired during the steady injection period have first been averaged for each experiment separately. Then, the mean images of the ten experiments of one series have been averaged again and those averaged images then serve as the basis of the following discussion.

The two images on the left side of Figure 20 show the spray of the reference case of the present measurement series (image a) compared with the reference case of earlier measurement series [17] without obstacle in the nozzle (image b). In both cases, the spray propagates without deflection from its nominal spray axis – defined by the orifice. However, in the case with obstacle, the overall spray angle is apparently increased.

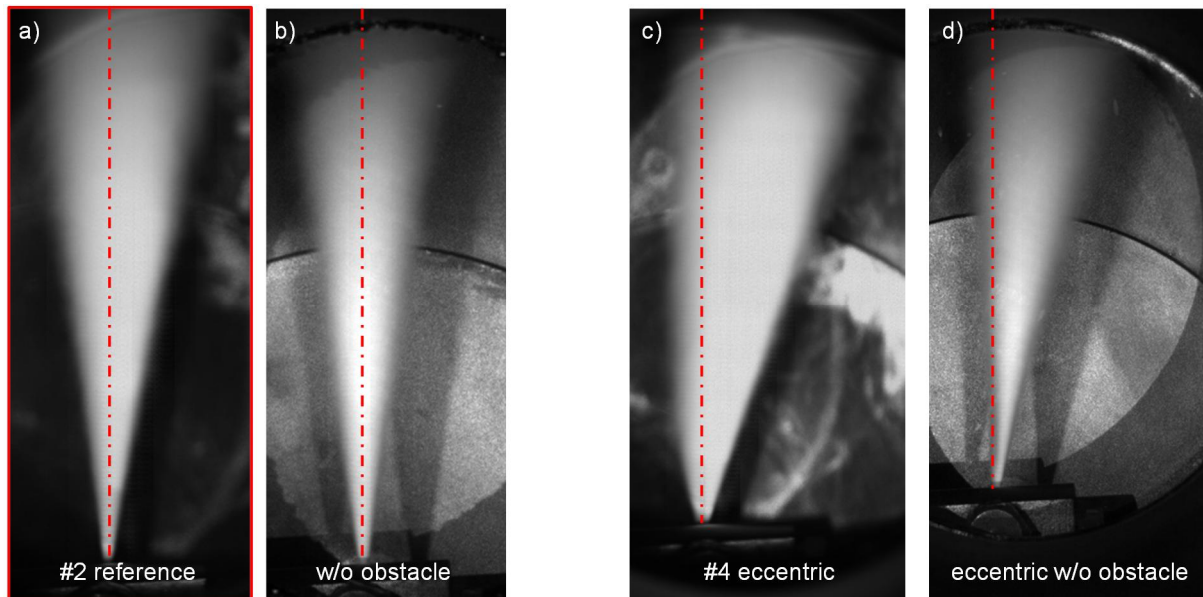


Figure 20: Comparison of the reference case with and without obstacle (left images) as well as the eccentric case with and without obstacle (right images)

The effect of nozzle-internal geometry features on spray characteristics is even more clearly visible when looking at the two cases shown on the right side of Figure 20. It shows again a comparison of two cases with and without insert; however with non-negligible eccentricity of the orifice (0.8) relative to the nozzle axis.

In case of an eccentric nozzle hole, the spray is significantly deflected against the direction of the eccentricity, which is the case for both sprays. Again, the presence of the insert in the flow passage underneath the orifice leads to an increased spray angle (comparing Figure 20 c to d), with the increase appearing to be even more pronounced than in the non-eccentric case. Moreover, the spray becomes clearly non-symmetric.

Figure 21 shows the averaged images for the five investigated cases. The reference case (nozzle #2) shows a symmetrical jet with a spray angle of about 20° . If the channel height s is reduced, as in nozzle #1, the spray is not influenced in lateral direction. The introduction of eccentricity on the other hand has a significant influence on the spray, as already discussed earlier.

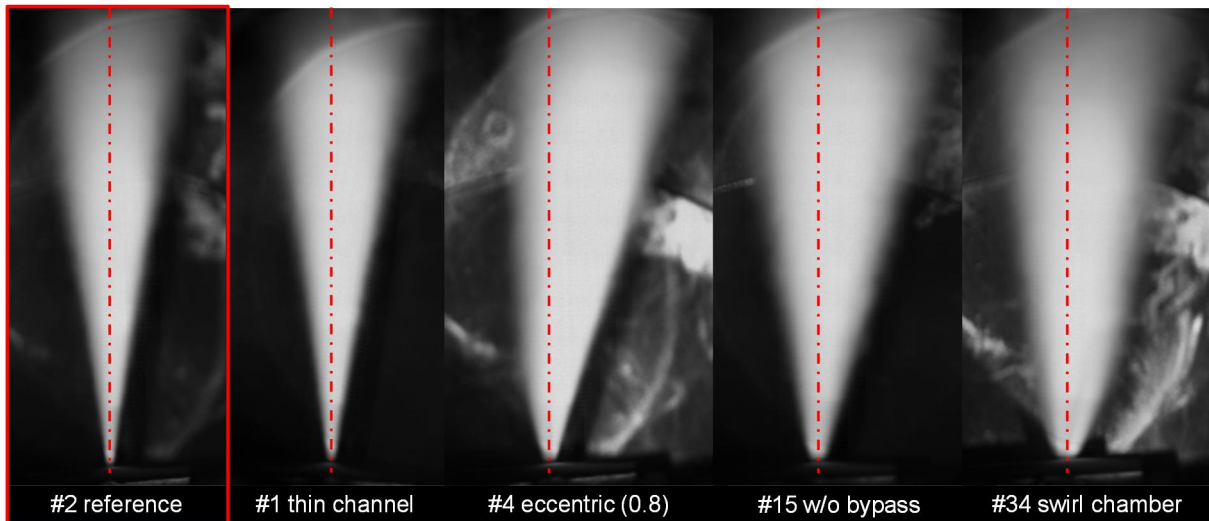


Figure 21: Spray images of the investigated nozzle designs, taken from the front and averaged during the steady phase.

In case of a nozzle without bypass, as in nozzle #15, the spray angle is increased compared to the reference case. It has to be stated here that the increase seen is not only the result of a drastically increased spray angle, but a combination of increased spray angle and an instable spray axis: From shot to shot, the spray axis of nozzle #15 stabilizes at one of two steady positions. Either the spray tilts 2° to the right or the left side of the theoretical spray axis. Statistically, the spray behaves such that it prefers the position on the right side, which is why the averaged image is pointing to the right.

The swirl chamber, as in nozzle #34 (Figure 21, right image) leads to a very broad spray. The swirl produced in the nozzle is transferred through the orifice and the vector components of the flow field pointing in tangential direction lead to a larger spray angle. Compared to the reference spray, the spray from the swirl chamber also shows a different spray shape. While for nozzles #2, #1 and #15 the shape is close to a triangle with more or less constant spray angle, nozzle #34 results in a shape which is very wide close to the nozzle, but with a change in the spray angle after a third of the total visible length. Note that such change of spray angle can also be observed in case of eccentricity, but here only on the left side, i.e. in the direction of the eccentricity.

Figure 18 shows the views from camera 2 on the side of the spray. Note that the dark zone in the middle of the spray is an artefact arising from the post processing of the images.

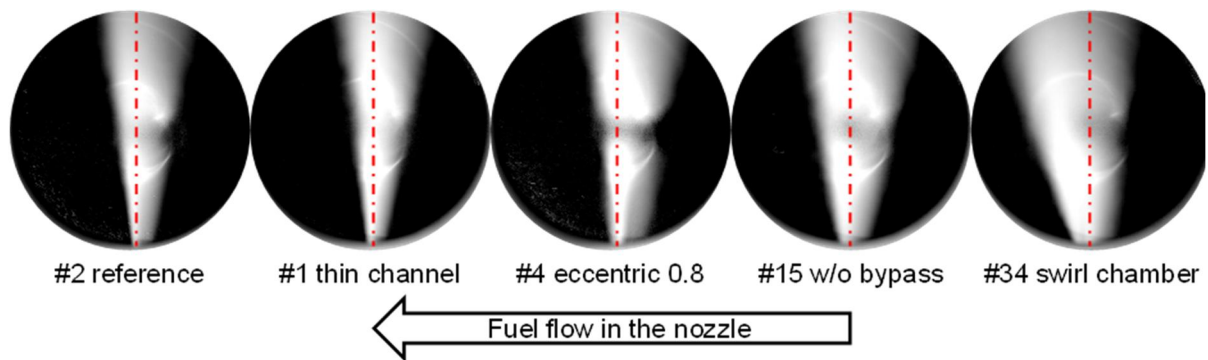


Figure 22: Spray images of the investigated nozzle designs, taken from the side and averaged during the steady phase

Nevertheless the images allow assessing the characteristics of the spray in axial direction: For the reference case, the spray is leaning backwards, against the direction of the fuel flow in the nozzle. For the case with a reduced height of the flow channel (nozzle #1) the spray is slightly wider yet very similar. But if an eccentricity is introduced the spray becomes wider, with a tendency against the flow direction in the nozzle. Interesting is the case without bypass, comparable to a single-hole nozzle: The spray becomes considerably wider than in the reference case and is also more symmetric, the leaning against the flow direction in the nozzle is less pronounced. For the swirl chamber, the flow becomes very wide, as was already observed from the front side. Moreover, it seems to be leaning more in the direction of the flow in the nozzle.

A closer investigation on the in nozzle flow, in combination with computational fluid dynamics can be found in [21]

6 Discussion, conclusion and outlook

The goals of this project were met, as the adaption of the Spray Combustion Chamber towards higher flexibility of the injection system was accomplished in the implementation of time controlled injection. Further the MED was improved in order to have a better repeatability and less fuel “consumption” of the system itself. Further it was possible to extend the application range of the measurement equipment, i.e. the PDA system was extended for the measurement of opaque fuels. And finally a small range of fuels was tested. The investigations performed during the FlexiFuel project focused on the following topics:

- In-nozzle flow
- Microscopic examination of the spray
- Ignition and combustion of different fuel qualities

The in-nozzle flow measurements conducted in earlier investigations have been extended in order to understand the influence of new nozzle designs on the flow field in the nozzle and the resulting spray breakup and spray morphology. These analyses were necessary as the car and truck industry, as well as most of the four-stroke industry, does not face problems like eccentric nozzles and therefore the interest of the international spray and combustion community is very limited. The investigations conducted in the FlexiFuel project – as well as in earlier projects supported by the Swiss Federal Office of Energy (SFOE) – resulted in answers, leading to new questions and new projects like the EccoMate project, where a PhD student looks with computational tools into the spray breakup of eccentric nozzles.



Another project, also with the highly appreciated support of the SFOE, is the INFLOSCOM project. During this venture a PhD student will work at the University of Chalmers and apply measurement techniques which are at the cutting edge of technology in order to get a better understanding of the relation between in-nozzle flow, cavitation and primary breakup and their influence on spray morphology, ignition and combustion.

Due to a very good collaboration between WinGD, ETH Zürich, PSI Villigen and EMPA Dübendorf, the “old” PDA system could be reactivated and improved. The system was applied in order to investigate the micro scale processes during secondary breakup. For the first time the spray of an injector representing the dimensions and injection pressure of a two-stroke marine diesel engine, was investigated under relevant pressure, temperature and flow conditions. Additionally a way to measure opaque fluids was developed and an HFO spray was investigated in a complex and time consuming series. The results of these investigations and further studies will be published in a PhD thesis in collaboration with ETH Zürich.

The development of an OH*-chemiluminescence method to determine between UV light from the OH radical and from the soot incandescence, as well as the media separator which allows the application of small, non conform fuel samples to the SCC, lead to investigations with new and unconventional fuels. Whithin these investigations new collaborations could be started with the Technical University Eindhoven and a SpinOff company, looking into new fuels for shipping. The investigations triggered also the participation of WinGD in the proposal of Falcon, a Horizon2020 project with the goal to build a mid scale plant to generate 2nd generation biofuels.

The investigations into the ignition and combustion also resulted contributions to the PhD thesis, as well as a paper at the SAE congress in Birmingham, UK.

It can therefore be said that – from the point of view of WinGD – the FlexiFuel project was highly successful, as it helped answering important questions in the field of spray and combustion of large marine diesel engines, supported the further collaboration between WinGD and the Swiss research partners, ETH Zürich, PSI Villigen, and EMPA Zürich, it also lead to several publications and triggered the start of new projects and collaborations.

The author would like to thank the Swiss Federal Office of Energy for its valuable contribution.

7 References

- [1] <http://www.hercules-2.com/>
- [2] Clarkson Research Services
- [3] <http://www.bunkerworld.com/prices/bunkerworldindex/>
- [4] Syha, M. & Schmid, A., „Future Fuels in Shipping“, internal Report WinGD, 2015
- [5] Herrmann, K., Schulz, K. and Weisser, G. „Development of a reference experiment for large diesel engine combustion system optimization“, CIMAC Congress 2007, Vienna, Austria
- [6] Herrmann K., Kyrtatos A., Schulz R., Weisser G., von Rotz B., Schneider B., Boulouchos K., “Validation and Initial Application of a Novel Spray Combustion Chamber Representative of Large Two-Stroke Diesel Engine Combustion Systems”, ICLASS 2009, Vail, Colorado USA.



- [7] Fankhauser, S., Heim, K., "The Sulzer RT-flex: Launching the era of common rail on low speed engines". CIMAC Congress 2001, Hamburg, Germany.
- [8] Schmid, A., BFE Jahresbericht 2012: Vertrags- und Projektnummer: 154269 / 103241
- [9] Wigley, G., Hargrave, G. K. , et al. (1998). "A high Power, High Resolution LDA/PDA System Applied to Dense Gasoline Direct Injection Sprays". 9th Int. Symposium on Applications of Laser Techniques to Fluid Mechanics. Lisbon, Portugal.
- [10]Schneider, B. (2003). „Experimentelle Untersuchung zur Spraystruktur in transienten, verdampfenden und nicht verdampfenden Brennstoffstrahlen unter Hochdruck“. P.h.D. thesis Diss. ETH Nr. 15004. Department of Mechanical and Process Engineering. Zürich, ETH Zürich
- [11]Hargrave, G. K, Wigley, G., Allen, J. and Bacon, A. "Optical Diagnostics and Direct Injection of Liquid Fuel Sprays", Journal of Visualization, Vol. 2, Nos. 3/4 (2000) 293-300
- [12]Schmid, A. (2012). „Experimental characterization of the two phase flow of a modern, piezo activated hollow cone injector“, DISS. ETH NO. 20852. Department of Mechanical and Process Engineering. Zürich, ETH Zürich
- [13]Kammermann T., "Droplet Characterization of HFO Sprays by Means of PDA", Master thesis, ETH Zürich, 2013
- [14]Schmid, A., Von Rotz B., Bombach, R., et al. „Ignition Behaviour of Marine Diesel Sprays“, COMODIA2012, Fukuoka, Japan
- [15]Schmid, A., Von Rotz, B., Weisser, G., and Herrmann, K., "Ignition Behaviour of Marine Diesel Fuels under Engine Like Conditions," SAE Technical Paper 2014-01-2656, 2014, doi:10.4271/2014-01-2656.
- [16]Eisentraut A., "Sustainable Production of Second Generation Biofuels - Potential and perspectives in major economies and developing countries", International Energy Agency, 2010
- [17]Schmid, A., von Rotz, B., Bombach, R., Weisser, G. and Herrmann, K., "Influence of nozzle hole eccentricity on spray morphology", ILASS-Europe 2013, Chania, Greece
- [18]Spahni, M., Kyrtatos, A., de Jong, R., "The New X Generation Low-Speed Engines from Wärtsilä", CIMAC Congress 2013, Shanghai, China
- [19]S. Hensel, K. Herrmann , R. Schulz and G. Weisser, "Numerical analysis and statistical description of the primary breakup in fuel nozzles of large two stroke engines for the application in CFD engine simulations", COMODIA 2012, July 23-26, 2012, Fukuoka, Japan.
- [20]R. Schulz, S. Hensel, B. von Rotz, A. Schmid, K. Herrmann, and G. Weisser, "Development of Spray and Combustion Simulation Tools and Application to Large Two-Stroke Diesel Engine Combustion Systems," in Proceedings of the Council International des Machines a Combustion (CIMAC) Congress, Shanghai, no. NO. 259, 2013.
- [21]A. Schmid, B. von Rotz, et al. Influence of in-nozzle flow on spray morphology, ILASS 2014, September 2014, Bremen, Germany



8 Publications within the FlexiFuel project

- B. von Rotz, T. Kammermann, et al., „[Evaluation of PDA Applicability in Regard to Heavy Fuel Oil Spray Investigations](#)”, 17th International Symposium on Applications of Laser Techniques to Fluid Mechanics Lisbon, Portugal, 07-10 July, 2014
- A. Schmid, B. von Rotz, et al., “[Influence of in-nozzle flow on spray morphology](#)”, ILASS 2014, September 2014, Bremen, Germany
- A. Schmid, B. Von Rotz, et al., "[Ignition Behaviour of Marine Diesel Fuels under Engine Like Conditions](#)", SAE Technical Paper 2014-01-2656, 2014, doi:10.4271/2014-01-2656.
- I. G. Nagy, A. Schmid, S. Hensel, “[Computational analysis of spray primary breakup in 2-stroke marine diesel engines with different nozzle layouts](#)”, ICLASS 2015, September 2015, Tainan, Taiwan

Yet to be published:

- B. von Rotz, PhD thesis, ETH Zürich
- B. von Rotz, Journal paper on Spray morphology for heavy fuels
- B. von Rotz, Journal paper on Ignition and Combustion